ORGANOMETALLICS

pubs.acs.org/Organometallics Article

Role of dppf Monoxide in the Transmetalation Step of the Suzuki–Miyaura Coupling Reaction

Pierre-Adrien Payard,* Antoine Bohn, Damien Tocqueville, Khaoula Jaouadi, Emile Escoude, Sanaa Ajig, Annie Dethoor, Geoffrey Gontard, Luca Alessandro Perego, Maxime Vitale, Ilaria Ciofini,* Simon Wagschal,* and Laurence Grimaud*

Cite This: *Organometallics* 2021, 40, 1120–1128 Read Online

ABSTRACT: Diphosphine ligands are frequently used in palladium-catalyzed Suzuki–Miyaura (S-M) reactions. Despite their widespread application in both academic and industrial settings, their role in the B-to-Pd transmetalation has not been firmly established. We combined electrochemistry, NMR spectroscopy, and DFT calculations to elucidate the role of dppf (1,1′-bis(diphenylphosphino)-ferrocene) in this key elementary step of the S-M reaction. We observed that excess dppf inhibits transmetalation involving $PhB(OH)_2$ and dppf-ligated arylpalladium(II) complexes, while an optimal [base]/[$PhB(OH)_2$] ratio maximizes the concentration of a [Pd–O–B] key intermediate. *In situ* oxidation of dppf to the diphosphine monoxide dppfO can take place in the presence of base, leading to dppfO-ligated arylpalladium(II) complexes, which readily undergo transmetalation at room temperature. These findings suggest guidelines for the rational optimization of diphosphine-promoted S-M reactions.

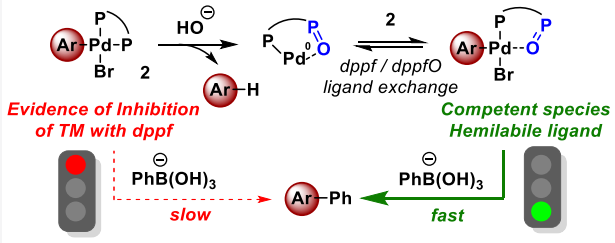

The metal-catalyzed cross-coupling of organoboron derivatives with electrophiles, known as the Suzuki–Miyaura (S-M) reaction, has become one of the most important synthetic transformations in modern organic chemistry.[1,2] It is widely applied on an industrial scale to manufacture active pharmaceutical ingredients and fine chemicals.[3] The mechanism of this reaction has been the subject of several experimental and theoretical studies.[4−7] As displayed in Scheme 1, it is generally admitted to involve three elementary steps: an oxidative addition (OA), a transmetalation (TM), and a reductive elimination (RE). As it generally limits the rate of the overall cross-coupling process, the TM step has been the subject of several thorough mechanistic studies.

Scheme 1. General Mechanism of the S-M Cross-Coupling Reaction

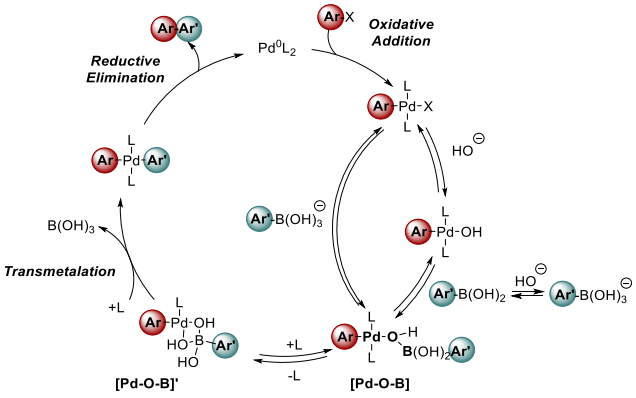

The TM can either proceed through the addition of the boronate $[Ar'B(OH)_3]^-$ to the OA product[5b,6a−d,g−k] or from the association of the boronic acid with the Pd hydroxo complex (Scheme 1).[5g−i,l] The rate of this step can be finely tuned by the base/boronic acid ratio,[5g,i,l] and the Denmark group gave the first experimental evidence of the key intermediate, the heterobimetallic [Pd–O–B] key species, which completed the description of the mechanistic scenario (Scheme 1).[5b,n,o,q]

Diphosphines such as 1,1′-bis(diphenylphosphino)ferrocene (dppf), 1,2-bis(diphenylphosphino)ethane (dppe), and 1,3-bis(diphenylphosphino)propane (dppp) are commonly used ligands in palladium-catalyzed Suzuki–Miyaura cross-couplings.[1k] The mechanistic picture emerging from existing studies, which have almost exclusively focused on monodentate phosphine ligands, is difficult to extend to chelating diphosphines in a straightforward manner.

Received: February 14, 2021
Published: April 12, 2021

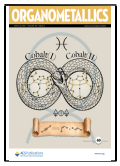

https://doi.org/10.1021/acs.organomet.1c00090
Organometallics 2021, 40, 1120–1128

In particular, a mechanistic model should explain how bidentate ligands can accommodate the formation of the key [Pd−O−B] and [Pd−O−B]′ species, both of which are necessary for the TM to occur according to the mechanism reported in Scheme 1. This issue has not been addressed systematically in the literature. Denmark and co-workers observed a slightly reduced transmetalation rate when dppf was employed instead of P*i*Pr$_3$ and conjectured the need of generating a coordinatively unsaturated intermediate,[5o] whose nature could not be firmly established. A theoretical study focusing on the S-M reaction promoted by complexes of the model ligand $H_2PCH_2CH_2PH_2$ investigated only an associative mechanism, for which very high energy barriers were computed.[6f]

These two reports and the frequent use of diphosphine ligands in S-M cross-couplings prompted us to investigate the B-to-Pd transmetalation in the case of diphosphines. We observed that the oxidation of dppf, a diphosphine widely used in S-M reactions applied to the total synthesis of natural products,[1] could take place under conditions mimicking a typical catalytic reaction, yielding the monoxide dppfO. Our results highlight the potentially crucial role of this *in situ* generated species in diphosphine-mediated S-M reactions (Scheme 2).[8]

Scheme 2. Hypothesis on the Tole of dppfO in S-M Reactions Proposed in This Paper

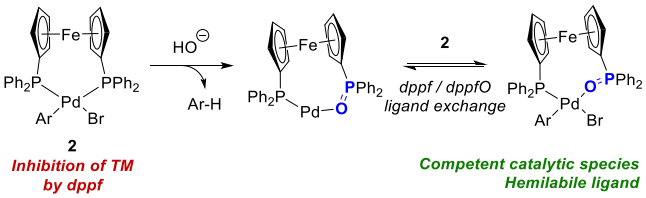

■ RESULTS AND DISCUSSION

The oxidative addition complex *cis*-[Pd^{II}(Ar)Br(dppf)] (**2**, Ar = 4-F-C$_6$H$_4$) was prepared by ligand exchange between *trans*-[Pd^{II}(Ar)Br(PPh$_3$)$_2$] (**1**) and dppf (Figure 1A) to study TM involving PhB(OH)$_2$ using tetrabutylammonium hydroxide (TBAOH) as a base.

Inhibiting Effect of Extra Diphosphine on the TM. We first investigated the effect of excess ligand on the B-to-Pd TM starting from either the OA complex **1** or **2** and different amounts of added PPh$_3$ or dppf. The ratio [OH$^-$]/[PhB(OH)$_2$] ≈ 0.6 (6 equiv/10 equiv) previously reported to maximize the TM rate in the case of PPh$_3$-ligated complexes was used.[5g] The formation of the coupling product Ar-Ph was monitored by ^{19}F{^{1}H} NMR spectroscopy (Figure 1B).[9]

In the case of complex **1** in the presence of additional PPh$_3$ (2 equiv), the coupling reaction was almost complete after 10 min (Figure S5a). Formation of Ar-Ph followed a first-order law with an apparent rate constant of k_{app} = 3.3 × 10^{-3} s^{-1}.[5g] No intermediate could be detected in this case, in agreement with TM being rate determining.[5g] In stark contrast, in the case of complex **2**, in the presence of 1 equiv of dppf (Figure 1B, green curve), TM was very slow and only 20% conversion was observed after 90 min. Under these conditions, the kinetics could be fitted by a first-order rate law and the apparent rate constant was estimated to be k_{app} = 3.2 × 10^{-5} s^{-1} (Figure S5d). The ratio between the two rate constants is about 100, which corresponds to a difference in activation energy of approximately 3 kcal mol^{-1}. These observations indicate that dppf strongly inhibits B-to-Pd transmetalation. The TM turns out to be the second elementary step of the S-M reaction to be inhibited by excess dppf, as it has been shown that extra diphosphine also inhibits OA by hampering the formation of the reactive 14-electron complex [Pd^0(dppf)].[11]

To rationalize these kinetic results, we estimated the energy barriers of the TM by DFT calculations (see the computational details in the Supporting Information) (Figure 1C and Figure S6). The slower TM rate with dppf in comparison to that with PPh$_3$ could possibly be due to a dissociative mechanism, in contrast with the working hypothesis previously formulated by Huang et al.[6f] Indeed, as first demonstrated by Goossen and Thiel,[6c] the TM with PPh$_3$-ligated Pd(II) requires partial phosphine decoordination and takes place via a four-centered transition state involving the concerted formation of a Pd−C bond and cleavage of Pd−B bonds. Similar behavior is predicted for dppf (Figure 1C and Figure S6).

With the complex [Pd−O−B] as the starting point (**A**), the cleavage of one P−Pd bond can be assisted by one OH of the boronate moiety to form complex **B**. This release is endothermic (+12.8 kcal mol^{-1}) and almost entropically neutral (+9.8 cal mol^{-1} K^{-1}), leading to an overall endergonic process. For comparison, the same process involving PPh$_3$ lies 2.6 kcal mol^{-1} lower in energy (+7.3 kcal mol^{-1}), driven by the strong positive entropic contribution (+59.3 cal mol^{-1} K^{-1}). Nonetheless, complex **B** cannot directly take part in TM since the phenyl moiety on the boron center is too far from the Pd center (d_{C-Pd} = 3.42 Å). Therefore, prior to TM a ligand exchange between the OH and Ph linked to the boron atom is required, leading to the formation of complex **C**. The two pre-TM complexes **C**-*cis* (+12.8 kcal mol^{-1}) and **C**-*trans* (+15.7 kcal mol^{-1}) can be formed depending on the relative position of the two aromatic rings with respect to the Pd center. For clarity, in the main text and figures we will refer only to the most stable *cis* conformer, while all data corresponding to the *trans* conformer are available in the Supporting Information. In the case of dppf, both isomers are 4−5 kcal mol^{-1} higher in free energy in comparison to the PPh$_3$ analogues. Finally, both *cis* and *trans* transition states were optimized, lying at 24.5 and 27.5 kcal mol^{-1}, respectively. The energy barrier for phosphine decoordination directly affects these transition states. In the case of PPh$_3$, the most favorable **TS**-*cis* was localized at +21.9 kcal mol^{-1}, i.e. about 3 kcal mol^{-1} lower in comparison to dppf, corresponding roughly to a factor of 10^2 on the kinetics of the reaction.[13] Both experimental and theoretical studies thus point toward a slower transmetalation rate when diphosphine ligands are used. However, when the formation of the coupling product Ar-Ph was monitored in the absence of added dppf, the reaction proceeded more quickly, and it was essentially complete after 30 min (Figure 1B, black curve). In the latter case, the kinetic curve of formation of Ar-Ph displayed an induction period, which is either typical of an autocatalytic reaction or hints at the *in situ* generation of an active species from a less reactive precursor.[10] The induction period varies from nearly 1 h at low base concentration to a few seconds at high base concentration (Figure S23). This is in agreement with the instantaneous reaction reported by Denmark and co-workers,[5n] as the TM was studied starting from complex **3** with 1 equiv of boronic acid (corresponding to [OH$^-$]/[PhB(OH)$_2$] = 1). Consistent with the concentration profiles (Figure 2C), this induction period probably results from the

https://doi.org/10.1021/acs.organomet.1c00090
Organometallics 2021, 40, 1120−1128

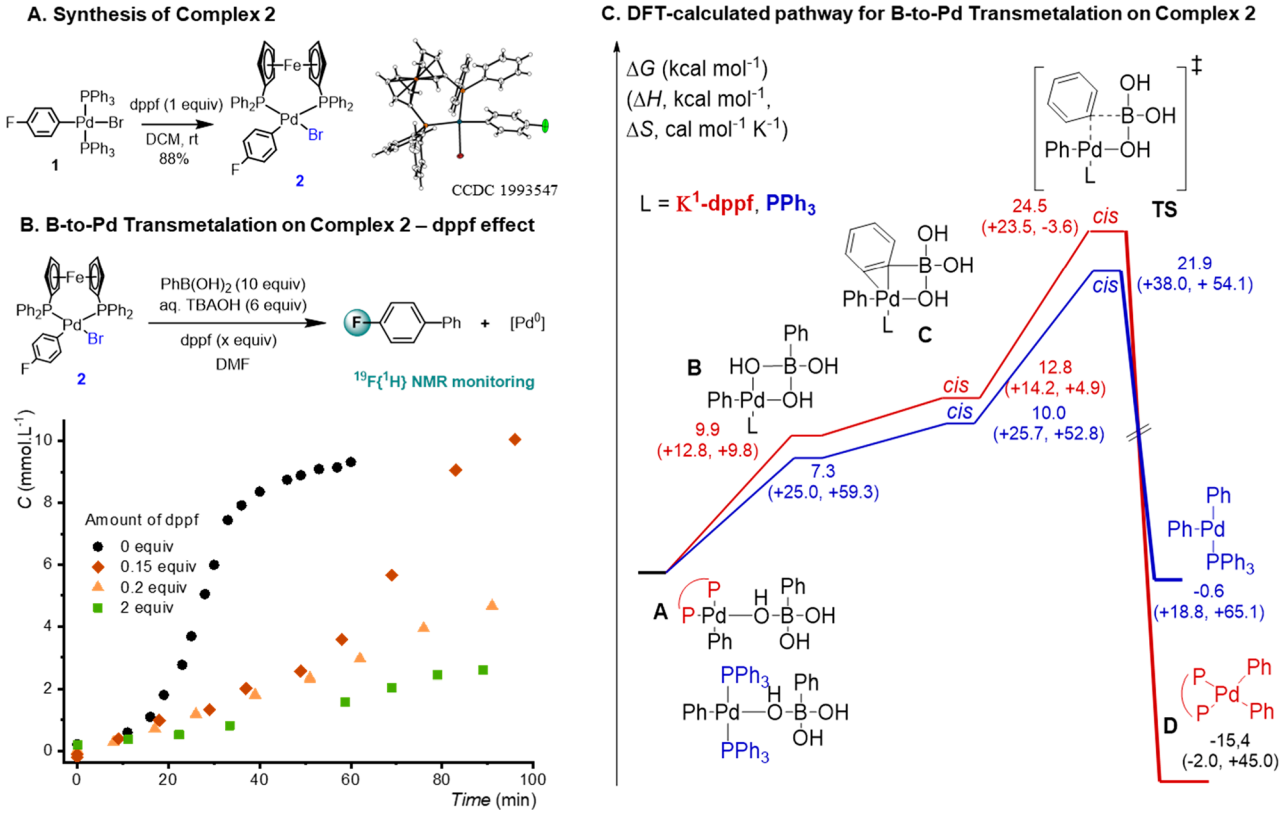

Figure 1. (A) Synthesis of complex **2** by ligand exchange from **1**. (B) Reaction monitoring of the formation of 4-fluoro-1,1′-biphenyl from **2** (20 mM in DMF) with $PhB(OH)_2$ (10 equiv) and 6 equiv of TBAOH (1.5 M in H_2O) at 20 °C, in the presence of varying amounts of dppf. (C) The most favored pathways for the TM and RE with dppf and PPh_3 as ligands (see Figure S6 for the alternative *trans* pathway), studied by DFT calculations. Computed relative Gibbs free energies are reported in kcal mol^{-1} at 298 K. Enthalpies (kcal mol^{-1}) and entropies (cal K^{-1} mol^{-1}) are reported in parentheses.

formation of a reactive species generated from either complex **3** or **4**. To shed light on this surprising behavior, we investigated in more detail the nature of the potential intermediates of the dppf-mediated S-M coupling.

Intermediates of the TM Step. When it is treated with TBAOH at −20 °C, complex **2**, characterized by its reduction potential R_2 at −1.75 V vs SCE in DMF, evolved to a new complex with a reduction peak R_3 at −2.2 V (Figure 2A and Figure S8). This new peak was assigned to the corresponding hydroxo complex $[Pd^{II}(Ar)(OH)(dppf)]$ (**3**), and the structure was confirmed by $^{31}P\{^1H\}$ and $^{19}F\{^1H\}$ NMR (Figures S9−S11).[5o] While the hydroxo complex **3** was stable at −20 °C, it rapidly decomposed at room temperature in the absence of $PhB(OH)_2$, thereby generating dppfO, as attested by CV showing the characteristic reduction peak of the latter compound (R_5 at −2.46 V vs SCE, Figure 2D). At the same time, the formation of fluorobenzene and 4-fluoro-1,1′-biphenyl was also observed by $^{19}F\{^1H\}$ NMR (Figures S10 and S24). In analogy with the well-described reduction of Pd(II) precatalysts in basic media,[12] complex **3** probably evolved through a reductive elimination to give dppfO-ligated Pd(0) along with the protodemetalation product Ar-H and the homocoupling product Ar-Ar, which were detected by $^{19}F\{^1H\}$ NMR (Figure 2D).[14]

When $PhB(OH)_2$ was added to the *in situ* generated $[Pd^{II}(Ar)(OH)(dppf)]$ (**3**), the new reduction peak R_4 was detected at −2.09 V vs SCE (Figure 2A). The latter was attributed to the formation of the mixed complex [Pd−O−B] (**4**), in analogy with the data reported by the Denmark group using *i*-Pr_3P as the ligand (Figures S12−S19).[5o] The $^{31}P\{^1H\}$ NMR titration of a solution containing complex **2** and 10 equiv of $PhB(OH)_2$ with TBAOH demonstrated that the optimal $[OH^-]/[PhB(OH)_2]$ ratio is about 0.5−0.6 so as to maximize the formation of the productive intermediate **4** (Figure 2B). It is worth noting that this optimal ratio can also vary depending on the quantity of boroxine present as an impurity in the boronic acid (Figures S20 and S21).[4b]

The TM process was monitored by $^{19}F\{^1H\}$ NMR using a ratio $[OH^-]/[PhB(OH)_2]$ = 0.5. Immediately after the addition of TBAOH, both **3** and **4** could be observed (Figure 2C, red curve), while some of the starting complex **2** remained (Figure 2C, blue curve). After an induction period of about 25 min, the cross-coupling product rapidly formed (Figure 2C, black curve). Interestingly, the additional intermediate Pd(II) complex **5** could be detected as a triplet at −124.4 ppm (Figure 2C, orange curve). Complex **5** accumulated during the reaction monitoring in parallel with a dramatic increase of the TM reaction rate (orange curve, Figure 2C). This behavior seems to point to complex **5** as being the active form of aryl-Pd toward transmetalation.

Role of Diphosphine Monoxide dppfO. To assess the potential catalytic role of dppfO or dppfO-ligated Pd species and shed light on the structure of complex **5**, the TM in the presence of 0.15 equiv of dppfO was studied (Figure 3B, purple curve). An induction period similar to that observed in the absence of additives was found (Figure 3B, blue curve). Importantly, the effect of extra dppfO is less pronounced than that of dppf (Figure 3B, green curve). This suggests that the

https://doi.org/10.1021/acs.organomet.1c00090
Organometallics 2021, 40, 1120−1128

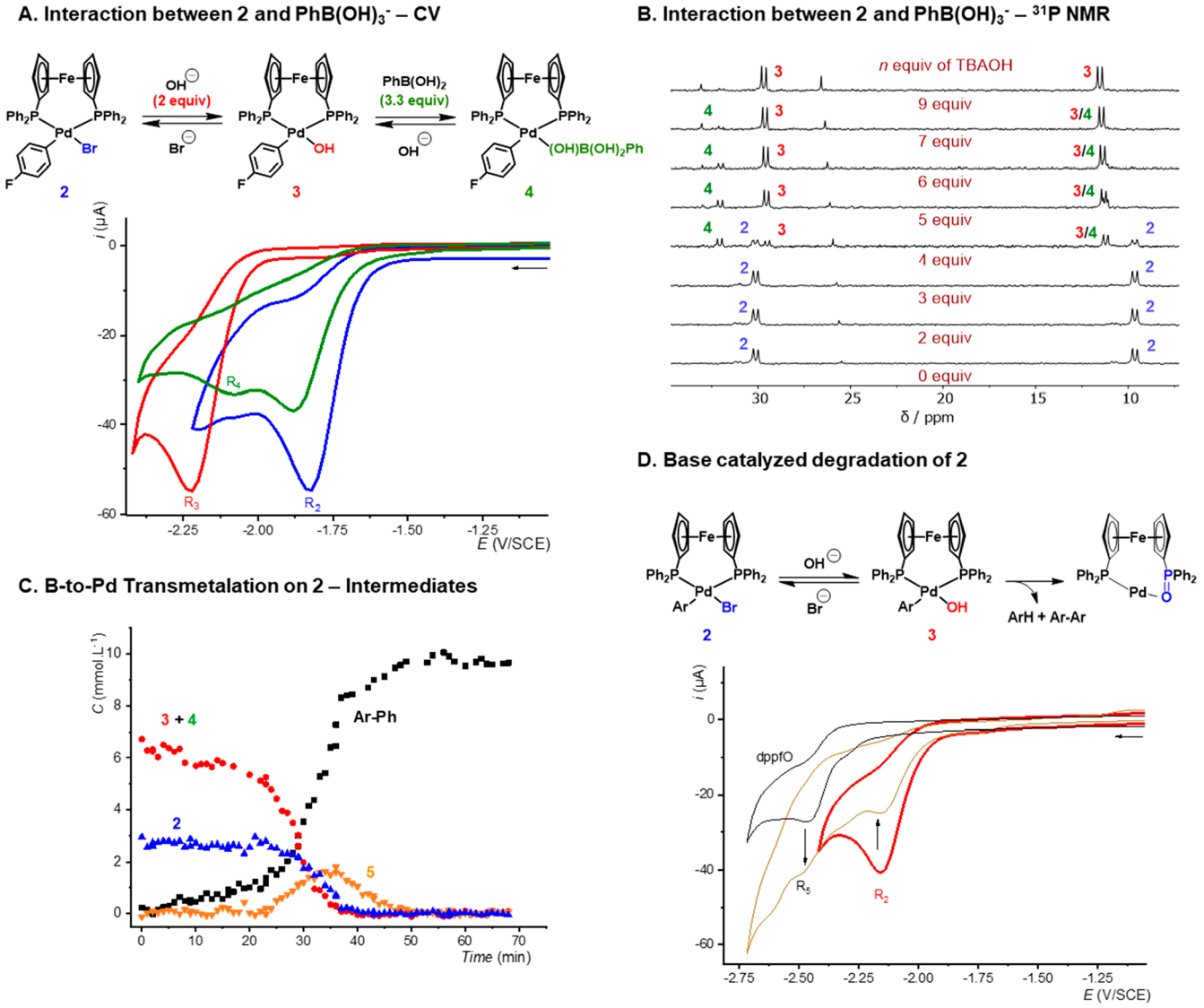

Figure 2. (A) CV performed toward the reduction potentials of a DMF solution containing 0.1 M of $TBABF_4$ at −20 °C at a scan rate of 0.2 V s^{-1} with **2** (2 mM) (blue), with 2 equiv of TBAOH (1.5 M in H_2O) (red), and after addition of $PhB(OH)_2$ (3.3 equiv corresponding to a ratio [base]/[boronic acid] of 0.6) (green). (B) $^{31}P\{^1H\}$ NMR of a solution of complex **2** (20 mM) in DMF in the presence of $PhB(OH)_2$ (10 equiv), upon increasing the amount of TBAOH (1.5 M in H_2O). A coaxial insert containing a solution of H_3PO_4 in DMSO-d_6 was used for locking and as an internal standard for integration. (C) Reaction monitoring of complex **2** (10 mM in DMF) with $PhB(OH)_2$ (10 equiv) in the presence of TBAOH (5 equiv) at 20 °C, monitored by $^{19}F\{^1H\}$ NMR. (D) Formation of dppfO from **2** and **3** (Ar = 4-F-C_6H_4). CV performed toward the reduction potentials of a DMF solution containing 0.1 M of $TBABF_4$ at rt, at a scan rate of 0.2 V s^{-1} with isolated complex **3** (2 mM (red) and after 4 min (brown) and CV of 2 mM of isolated dppfO (black).

addition of dppfO alone does not lead to an active species. When 0.1 equiv of $Pd^0(dba)_2$ was introduced (with or without 0.1 equiv of dppfO; Figure 3B, black and brown curves), no induction period could be detected and both reactions were complete within less than 20 min. In both cases, the protodemetalation product Ar-H and the homocoupling product Ar-Ar were observed, suggesting the concomitant decomposition of **3**.

We hypothesized that the presence of Pd(0) promotes the dppf/dppfO ligand exchange to form the less coordinated dppfO-ligated aryl-Pd(II) complex. When *in situ* generated $[Pd^0(dppfO)_2]$ (prepared by mixing $Pd^0(dba)_2$ and dppfO, *vide infra*) was added to a DMF solution of complex **2**, the $^{31}P\{^1H\}$ spectrum was quite complex, most probably due to a rapid exchange of ligands on the NMR time scale, but the signal corresponding to complex **5** was clearly observed by $^{19}F\{^1H\}$ NMR (Figure S31) and no induction period was apparent in this case (Figure 3B). This suggested that complex **5** is the active complex for TM and that it is formed in the presence of dppfO-ligated Pd^0.

A CV analysis of a mixture $Pd^0(dba)_2$ with 2 equiv of dppfO demonstrated that a stoichiometric amount of dppfO was able to displace all of the dba from the coordination sphere of Pd(0) (Figures S25−S27), thus suggesting a strong affinity of dppfO for Pd(0). This contrasts with what was observed with dppf, since the addition of 2 equiv of dppf on $Pd^0(dba)_2$ resulted in the formation of the mixed complex $[Pd^0(dba)(dppf)]$ (Figure S28).[11a] The resulting $[Pd^0(dppfO)_2]$ was characterized for the first time by $^{31}P\{^1H\}$ NMR (Figure S29) and by CV (oxidation peak O_1 at +0.5 V vs SCE). This peak disappeared after addition of an excess of 4-F-C_6H_4Br, confirming that this Pd(0) species is able to perform the

https://doi.org/10.1021/acs.organomet.1c00090
Organometallics 2021, 40, 1120−1128

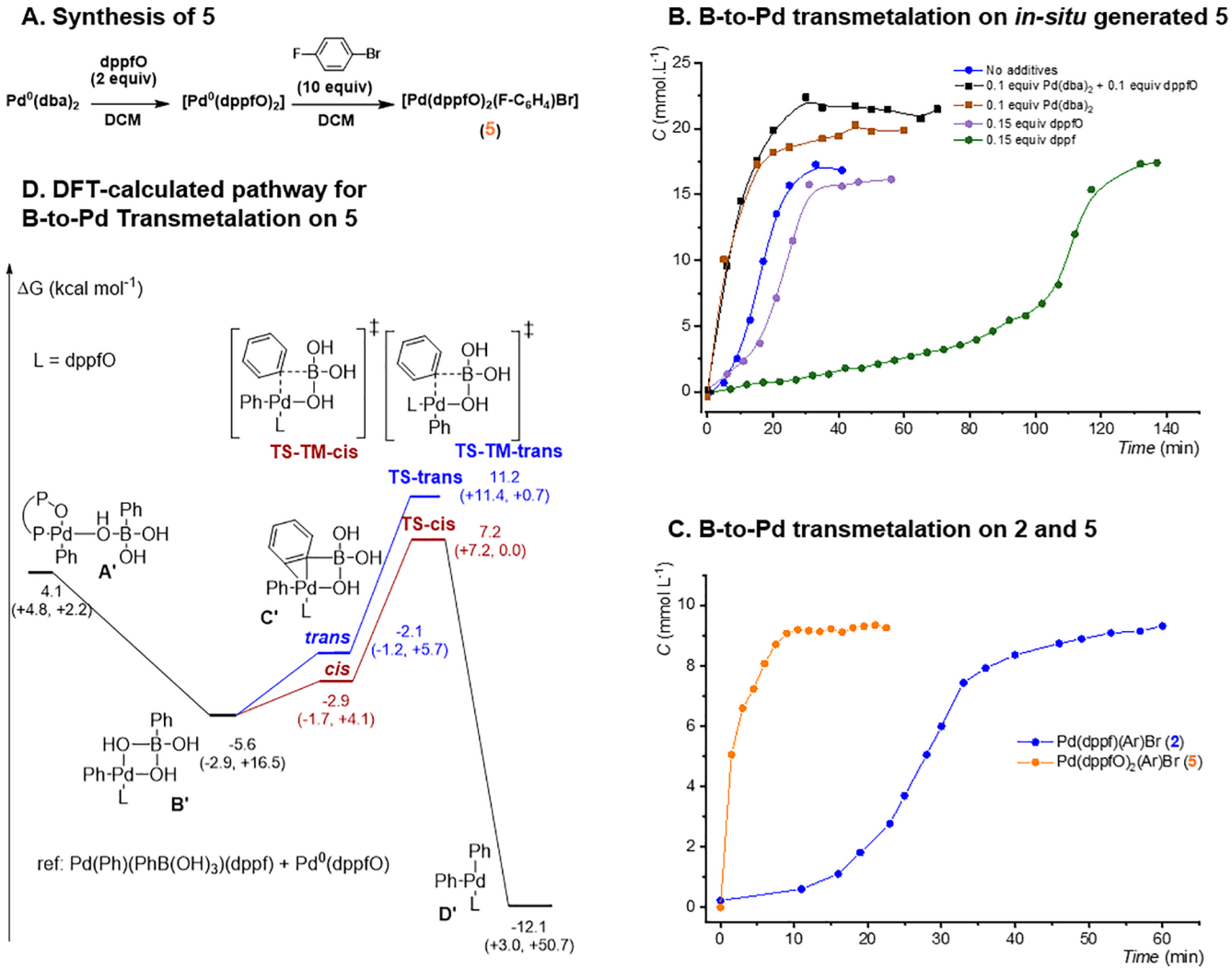

Figure 3. (A) Oxidative addition with $Pd^0(dppfO)_2$. (B) $^{19}F\{^1H\}$ NMR monitoring of the formation of 4-fluoro-1,1′-biphenyl from **2** (20 mM in DMF) with 10 equiv of $PhB(OH)_2$ and 6 equiv of TBAOH at 20 °C. (C) $^{19}F\{^1H\}$ NMR monitoring of the formation of 4-fluoro-1,1′-biphenyl from **2** (blue, 10 mM in DMF) and **5** (orange, 10 mM in DMF), both with 10 equiv of $PhB(OH)_2$ and 6 equiv of TBAOH at 20 °C. (D) Pathway for the TM process with dppfO as the ligand studied by DFT calculations. Computed relative Gibbs free energies are reported in kcal mol^{-1} at 298 K. Enthalpies (kcal mol^{-1}) and entropies (cal K^{-1} mol^{-1}) are reported in parentheses.

initial OA step (Figure S30).[15] $[Pd^{II}(Ar)Br(dppfO)_2]$ could be prepared and characterized by ^1H, ^{13}C, $^{19}F\{^1H\}$, and $^{31}P\{^1H\}$ NMR and by ESI-MS (Figure 3A and Figure S2−4). Spectral data of this complex were identical with those of the previously observed complex **5** (*vide supra*, Intermediates of the TM Step), which kinetics data indicated as a crucial intermediate. When isolated complex **5** was treated with $PhB(OH)_2$ and TBAOH, no induction period was observed and the TM was completed within 10 min (Figure 3C and Figure S32).

DFT calculations further confirmed that TM is favored with dppfO in comparison to TM with dppf (Figure 3D versus Figure 1D). In agreement with the experimental results, the ligand exchange reaction between $[Pd^0(dppfO)]$ and the dppf-ligated [Pd−O−B] to form dppfO-ligated complex **A′** is only slightly endergonic (+4.1 kcal mol^{-1}) and the formation of complex **B′** is favored (−9.7 kcal mol^{-1}). Coordination of the aromatic moiety to form complexes *cis*- or *trans*-**C′** is even more favorable, and as expected, the transition states for the TM step are very low lying (+7.2 and +11.2 kcal mol^{-1} for the *cis* and *trans* isomers, respectively), accounting for the high activity of hemilabile-ligated Pd species for TM. Additionally, the RE step was also predicted to be faster with monocoordinated dppfO-ligated Pd species in comparison to the dppf analogue (Figure S35).

■ CONCLUSIONS

This work addressed three key points regarding the use of diphosphine ligands in the Suzuki-Miyaura reaction concerning (i) their effect on TM rate, (ii) the need for decoordination prior to TM, and (iii) the possible inhibitory effects of diphosphine ligands. In the course of our study, we observed that TM involving $[Pd^{II}ArBr(dppf)]$ and $PhB(OH)_2$ in the presence of OH^- proceeds with an induction period, suggesting that this complex needs to be converted to a more reactive species, which could be the actual intermediate of the catalytic cycle in S-M reactions. We have proved that dppf actually inhibits the TM, and DFT calculations pointed out the need of partial decoordination of dppf for the TM to occur. Moreover, we showed that the dppfO generated from the *in situ* oxidation of dppf has a high affinity for Pd(0) species. $Pd^0(dppfO)_2$ is able to perform oxidative addition to ArBr to give a dppfO-ligated aryl-Pd(II), which in turn is very

https://doi.org/10.1021/acs.organomet.1c00090
Organometallics 2021, 40, 1120−1128

reactive in the TM with $PhB(OH)_2$, as confirmed both experimentally and theoretically.

Finally, this study accounts for the widespread use of $[Pd^{II}(dppf)Cl_2]$ as a precatalyst for Suzuki–Miyaura cross-couplings, which is a direct precursor of dppfO-ligated Pd(0). The diphosphine ligand is required for the reduction of most commercially available Pd(II) precatalysts,[12] but diphosphine monoxides could constitute efficient ligands to stabilize Pd(0) species and promote both the oxidative addition and the transmetalation steps.

■ COMPUTATIONAL DETAILS

All DFT calculations were performed using the Gaussian 09 program (Rev. A02).[16] The structures of all minima and transition states were optimized using the M06 functional[17] and the following basis sets: 6-31G for C, H, F, and B; 6-31+G(d) for O and P; LANL2DZ for Pd and Fe with the associated effective core potential LANL2.[18] Bulk solvent effects were taken into account using the PCM method as implemented in Gaussian.[19] The default cavity parameters and static and optical dielectric constants for DMF were used. The nature of all stationary points was checked by analytical frequency calculations. Computed harmonic frequencies were employed to calculate free energies at 298 K and 1 atm pressure with the usual approximations.

■ EXPERIMENTAL SECTION

Synthesis of $[Pd^0(dppfO)_2(4\text{-}F\text{-}C_6H_4)(Br)]$ (5). The reaction was carried out under argon. To a stirred mixture of $[Pd^0(dba)_2]$ (50 mg, 0.087 mmol) in degassed CH_2Cl_2 (5 mL) were added 1-bromo-4-fluorobenzene (95 μL, 0.7 mmol) and 2.1 equiv of dppfO[20] (104 mg, 0.18 mmol). After vigorous stirring at ambient temperature (red-brown solution), the flask was fitted with a reflux condenser and heated in an oil bath at 50 °C overnight. The reaction mixture was warmed to room temperature, an then the solution was evaporated to a volume of approximately 1 mL and treated with degassed petroleum ether (5 mL). The dark red precipitate was filtered underan inert atmosphere, washed with petroleum ether, and dried *in vacuo* to produce complex **5** (100 mg, 80%). $^{31}P\{^1H\}$ NMR (121 MHz, DMF): δ 25.3 (br s), 16.1 (d, J_{P^-F} = 3.0 Hz) ppm. $^{19}F\{^1H\}$ NMR (282 MHz, DMF): δ = −124.4 (t, J_{P-F} = 3.0 Hz) ppm. MS (ESI+, MeCN) m/z (%): 1341.1 (100) $[(M - Br)^+]$.

■ ASSOCIATED CONTENT

Supporting Information

The Supporting Information is available free of charge at https://pubs.acs.org/doi/10.1021/acs.organomet.1c00090.

Cartesian geometries and absolute energies (XYZ)

Experimental ^{31}P NMR chemical shifts and calculated shielding constants and additional data on the effect of computational parameters on structures and shielding constants (PDF)

Accession Codes

CCDC 1993547 contains the supplementary crystallographic data for this paper. These data can be obtained free of charge via www.ccdc.cam.ac.uk/data_request/cif, or by emailing data_request@ccdc.cam.ac.uk, or by contacting The Cambridge Crystallographic Data Centre, 12 Union Road, Cambridge CB2 1EZ, UK; fax: +44 1223 336033.

■ AUTHOR INFORMATION

Corresponding Authors

Pierre-Adrien Payard − *Laboratoire des Biomolécules, LBM, Département de Chimie, École Normale Supérieure, PSL University, Sorbonne Université, CNRS, 75005 Paris, France;* orcid.org/0000-0001-5661-6128; Email: pierre-adrien.payard@univ-lyon1.fr

Ilaria Ciofini − *PSL University, Institute of Chemistry for Health and Life Sciences, I-CLeHS, CNRS-Chimie ParisTech, F-75005 Paris, France;* orcid.org/0000-0002-5391-4522; Email: ilaria.ciofini@chimie-paris.psl.eu

Simon Wagschal − *Discovery Product Development and Supply, Janssen Pharmaceutica, 8200 Schaffhausen, Switzerland;* orcid.org/0000-0003-1979-5838; Email: swagscha@its.jnj.com

Laurence Grimaud − *Laboratoire des Biomolécules, LBM, Département de Chimie, École Normale Supérieure, PSL University, Sorbonne Université, CNRS, 75005 Paris, France;* orcid.org/0000-0003-3904-1822; Email: laurence.grimaud@ens.psl.eu

Authors

Antoine Bohn − *Laboratoire des Biomolécules, LBM, Département de Chimie, École Normale Supérieure, PSL University, Sorbonne Université, CNRS, 75005 Paris, France*

Damien Tocqueville − *Laboratoire des Biomolécules, LBM, Département de Chimie, École Normale Supérieure, PSL University, Sorbonne Université, CNRS, 75005 Paris, France*

Khaoula Jaouadi − *Laboratoire des Biomolécules, LBM, Département de Chimie, École Normale Supérieure, PSL University, Sorbonne Université, CNRS, 75005 Paris, France*

Emile Escoude − *Laboratoire des Biomolécules, LBM, Département de Chimie, École Normale Supérieure, PSL University, Sorbonne Université, CNRS, 75005 Paris, France*

Sanaa Ajig − *Laboratoire des Biomolécules, LBM, Département de Chimie, École Normale Supérieure, PSL University, Sorbonne Université, CNRS, 75005 Paris, France*

Annie Dethoor − *Laboratoire des Biomolécules, LBM, Département de Chimie, École Normale Supérieure, PSL University, Sorbonne Université, CNRS, 75005 Paris, France*

Geoffrey Gontard − *Institut Parisien de Chimie Moléculaire, CNRS UMR 8232, Sorbonne Université, 75252 Paris, France*

Luca Alessandro Perego − *Discovery Product Development and Supply, Janssen Pharmaceutica, 8200 Schaffhausen, Switzerland;* orcid.org/0000-0002-6502-3268

Maxime Vitale − *Laboratoire des Biomolécules, LBM, Département de Chimie, École Normale Supérieure, PSL University, Sorbonne Université, CNRS, 75005 Paris, France;* orcid.org/0000-0002-6740-2472

Complete contact information is available at: https://pubs.acs.org/10.1021/acs.organomet.1c00090

Notes

The authors declare no competing financial interest.

■ ACKNOWLEDGMENTS

P.-A.P. is grateful to the ENS Paris Saclay and Solvay for a Ph.D. grant. We acknowledge Dr. D. Lesage for the mass spectrometry analyses. K.J. thanks ANR-17-CE07-0018 Hyper-Silight for Ph.D. grant. We thank Prof. A. Boutin, P. J. Yao, and Dr. Q. Chen for useful discussions. We thank Janssen Pharmaceutica and Bristol-Myers Squibb for funding the project.

■ REFERENCES

(1) (a) Miyaura, N.; Suzuki, A. Palladium-Catalyzed Cross-Coupling Reactions of Organoboron Compounds. *Chem. Rev.* **1995**, *95*, 2457−2483. (b) Negishi, E.-i. *Handbook of Organopalladium Chemistry for*

Organic Synthesis; Wiley: 2002. (c) Suzuki, A. Cross-coupling reactions via organoboranes. *J. Organomet. Chem.* **2002**, *653*, 83−90. (d) Miyaura, N., Organoboron Compounds. In *Cross-Coupling Reactions: A Practical Guide*; Miyaura, N., Ed.; Springer Berlin Heidelberg: 2002; pp 11−59. (e) Tsuji, J. *Palladium Reagents and Catalysts*; Wiley: 2004. (f) de Meijere, A.; Diederich, F. *Metal-Catalyzed Cross-Coupling Reactions*; Wiley-VCH: 2004. (g) Bellina, F.; Carpita, A.; Rossi, R. Palladium Catalysts for the Suzuki Cross-Coupling Reaction: An Overview of Recent Advances. *Synthesis* **2004**, *2004*, 2419−2440. (h) Martin, R.; Buchwald, S. L. Palladium-Catalyzed Suzuki−Miyaura Cross-Coupling Reactions Employing Dialkylbiaryl Phosphine Ligands. *Acc. Chem. Res.* **2008**, *41*, 1461−1473. (i) Li, H.; Johansson Seechurn, C. C. C.; Colacot, T. J. Development of Preformed Pd Catalysts for Cross-Coupling Reactions, Beyond the 2010 Nobel Prize. *ACS Catal.* **2012**, *2*, 1147−1164. (j) Johansson Seechurn, C. C. C.; Kitching, M. O.; Colacot, T. J.; Snieckus, V. Palladium-Catalyzed Cross-Coupling: A Historical Contextual Perspective to the 2010 Nobel Prize. *Angew. Chem., Int. Ed.* **2012**, *51*, 5062−5085. (k) Rossi, R.; Bellina, F.; Lessi, M.; Manzini, C.; Marianetti, G.; Perego, L. A. Recent Applications of Phosphane-based Palladium Catalysts in Suzuki-Miyaura Reactions Involved in Total Syntheses of Natural Products. *Curr. Org. Chem.* **2015**, *19* (14), 1302−1409. (l) Maluenda, I.; Navarro, O. Recent Developments in the Suzuki-Miyaura Reaction: 2010−2014. *Molecules* **2015**, *20*, 7528−7557.

(2) (a) Montgomery, J. Nickel-Catalyzed Reductive Cyclizations and Couplings. *Angew. Chem., Int. Ed.* **2004**, *43* (30), 3890−3908. (b) Han, F.-S. Transition-metal-catalyzed Suzuki−Miyaura cross-coupling reactions: a remarkable advance from palladium to nickel catalysts. *Chem. Soc. Rev.* **2013**, *42* (12), 5270−5298. (c) Yamaguchi, J.; Muto, K.; Itami, K. Recent Progress in Nickel-Catalyzed Biaryl Coupling. *Eur. J. Org. Chem.* **2013**, *2013* (1), 19−30. (d) Tasker, S. Z.; Standley, E. A.; Jamison, T. F. Recent advances in homogeneous nickel catalysis. *Nature* **2014**, *509* (7500), 299−309. (e) Ananikov, V. P. Nickel: The "Spirited Horse" of Transition Metal Catalysis. *ACS Catal.* **2015**, *5* (3), 1964−1971. (f) Li, Z.; Liu, L. Recent advances in mechanistic studies on Ni catalyzed cross-coupling reactions. *Chin. J. Catal.* **2015**, *36* (1), 3−14.

(3) (a) Magano, J.; Dunetz, J. R. Large-Scale Applications of Transition Metal-Catalyzed Couplings for the Synthesis of Pharmaceuticals. *Chem. Rev.* **2011**, *111* (3), 2177−2250. (b) Ashworth, I. W.; Campbell, A. D.; Cherryman, J. H.; Clark, J.; Crampton, A.; Eden-Rump, E. G. B.; Evans, M.; Jones, M. F.; McKeever-Abbas, S.; Meadows, R. E.; Skilling, K.; Whittaker, D. T. E.; Woodward, R. L.; Inglesby, P. A. Process Development of a Suzuki Reaction Used in the Manufacture of Lanabecestat. *Org. Process Res. Dev.* **2018**, *22* (12), 1801−1808. (c) Maity, P.; Reddy, V. V. R.; Mohan, J.; Korapati, S.; Narayana, H.; Cherupally, N.; Chandrasekaran, S.; Ramachandran, R.; Sfouggatakis, C.; Eastgate, M. D.; Simmons, E. M.; Vaidyanathan, R. Development of a Scalable Synthesis of BMS-978587 Featuring a Stereospecific Suzuki Coupling of a Cyclopropane Carboxylic Acid. *Org. Process Res. Dev.* **2018**, *22* (7), 888−897. (d) Schäfer, G.; Fleischer, T.; Ahmetovic, M.; Abele, S. Development of a Scalable Route for a Key Thiadiazole Building Block via Sequential Sandmeyer Bromination and Room-Temperature Suzuki−Miyaura Coupling. *Org. Process Res. Dev.* **2020**, *24* (2), 228−234. (e) Chen, C.-Y.; Dagneau, P.; Grabowski, E. J. J.; Oballa, R.; O'Shea, P.; Prasit, P.; Robichaud, J.; Tillyer, R.; Wang, X. Practical Asymmetric Synthesis of a Potent Cathepsin K Inhibitor. Efficient Palladium Removal Following Suzuki Coupling. *J. Org. Chem.* **2003**, *68* (7), 2633−2638. (f) Conlon, D. A.; Drahus-Paone, A.; Ho, G.-J.; Pipik, B.; Helmy, R.; McNamara, J. M.; Shi, Y.-S.; Williams, J. M.; Macdonald, D.; Deschênes, D.; Gallant, M.; Mastracchio, A.; Roy, B.; Scheigetz, J. Process Development and Large-Scale Synthesis of a PDE4 Inhibitor. *Org. Process Res. Dev.* **2006**, *10* (1), 36−45. (g) Li, B.; Buzon, R. A.; Zhang, Z. Syntheses of 4,5-Disubstituted Oxazoles via Regioselective C-4 Bromination. *Org. Process Res. Dev.* **2007**, *11* (6), 951−955. (h) Keen, S. P.; Cowden, C. J.; Bishop, B. C.; Brands, K. M. J.; Davies, A. J.; Dolling, U. H.; Lieberman, D. R.; Stewart, G. W. Practical Asymmetric Synthesis of a Non-Peptidic $\alpha_v\beta_3$ Antagonist. *J. Org. Chem.* **2005**, *70* (5), 1771−1779.

(4) For reviews dedicated to transmetalation see: (a) Partyka, D. V. Transmetalation of Unsaturated Carbon Nucleophiles from Boron-Containing Species to the Mid to Late d-Block Metals of Relevance to Catalytic C−X Coupling Reactions (X = C, F, N, O, Pb, S, Se, Te). *Chem. Rev.* **2011**, *111* (3), 1529−1595. (b) Lennox, A. J. J.; Lloyd-Jones, G. C. Transmetalation in the Suzuki−Miyaura Coupling: The Fork in the Trail. *Angew. Chem., Int. Ed.* **2013**, *52* (29), 7362−7370.

(5) Experimental mechanistic studies about Pd-catalyzed S-M coupling: (a) Aliprantis, A. O.; Canary, J. W. Observation of Catalytic Intermediates in the Suzuki Reaction by Electrospray Mass Spectrometry. *J. Am. Chem. Soc.* **1994**, *116*, 6985−6986. (b) Matos, K.; Soderquist, J. A. Alkylboranes in the Suzuki−Miyaura Coupling: Stereochemical and Mechanistic Studies. *J. Org. Chem.* **1998**, *63*, 461−470. (c) Adamo, C.; Amatore, C.; Ciofini, I.; Jutand, A.; Lakmini, H. Mechanism of the Palladium-Catalyzed Homocoupling of Arylboronic Acids: Key Involvement of a Palladium Peroxo Complex. *J. Am. Chem. Soc.* **2006**, *128*, 6829−6836. (d) Nunes, C. M.; Monteiro, A. L. Pd-catalyzed Suzuki cross-Coupling reaction of bromostilbene: insights on the nature of the boron Species. *J. Braz. Chem. Soc.* **2007**, *18*, 1443−1447. (e) Sicre, C.; Braga, A. A. C.; Maseras, F.; Cid, M. M. Mechanistic insights into the transmetalation step of a Suzuki−Miyaura reaction of 2(4)-bromopyridines: characterization of an intermediate. *Tetrahedron* **2008**, *64*, 7437−7443. (f) Butters, M.; Harvey, J. N.; Jover, J.; Lennox, A. J. J.; Lloyd-Jones, G. C.; Murray, P. M. Aryl Trifluoroborates in Suzuki-Miyaura Coupling: The Roles of Endogenous Aryl Boronic Acid and Fluoride. *Angew. Chem., Int. Ed.* **2010**, *49*, 5156−5160. (g) Amatore, C.; Jutand, A.; Le Duc, G. Kinetic Data for the Transmetalation/Reductive Elimination in Palladium-Catalyzed Suzuki−Miyaura Reactions: Unexpected Triple Role of Hydroxide Ions Used as Base. *Chem. - Eur. J.* **2011**, *17* (8), 2492−2503. (h) Carrow, B. P.; Hartwig, J. F. Distinguishing Between Pathways for Transmetalation in Suzuki−Miyaura Reactions. *J. Am. Chem. Soc.* **2011**, *133* (7), 2116−2119. (i) Amatore, C.; Jutand, A.; Le Duc, G. Mechanistic Origin of Antagonist Effects of Usual Anionic Bases (OH−, CO32−) as Modulated by their Countercations (Na+, Cs+, K+) in Palladium-Catalyzed Suzuki−Miyaura Reactions. *Chem. - Eur. J.* **2012**, *18* (21), 6616−6625. (j) Amatore, C.; Jutand, A.; Le Duc, G. The Triple Role of Fluoride Ions in Palladium-Catalyzed Suzuki-Miyaura Reactions: Unprecedented Transmetalation from [ArPdFL2] Complexes. *Angew. Chem.* **2012**, *124*, 1408−1411. (k) Amatore, C.; Jutand, A.; Le Duc, G. The Triple Role of Fluoride Ions in Palladium-Catalyzed Suzuki−Miyaura Reactions: Unprecedented Transmetalation from [ArPdFL2] Complexes. *Angew. Chem., Int. Ed.* **2012**, *51* (6), 1379−1382. (l) Amatore, C.; Le Duc, G.; Jutand, A. Mechanism of palladium-catalyzed Suzuki-Miyaura reactions: multiple and antagonistic roles of anionic "bases" and their countercations. *Chem. - Eur. J.* **2013**, *19*, 10082−93. (m) Fyfe, J. W. B.; Valverde, E.; Seath, C. P.; Kennedy, A. R.; Redmond, J. M.; Anderson, N. A.; Watson, A. J. B. Speciation Control During Suzuki-Miyaura Cross-Coupling of Haloaryl and Haloalkenyl MIDA Boronic Esters. *Chem. - Eur. J.* **2015**, *21*, 8951−8964. (n) Thomas, A. A.; Denmark, S. E. Pre-transmetalation intermediates in the Suzuki-Miyaura reaction revealed: The missing link. *Science* **2016**, *352*, 329−332. (o) Thomas, A. A.; Wang, H.; Zahrt, A. F.; Denmark, S. E. Structural, Kinetic, and Computational Characterization of the Elusive Arylpalladium(II)boronate Complexes in the Suzuki−Miyaura Reaction. *J. Am. Chem. Soc.* **2017**, *139*, 3805−3821. (p) Kohlmann, J.; Braun, T.; Laubenstein, R.; Herrmann, R. Suzuki-Miyaura Cross-Coupling Reactions of Highly Fluorinated Arylboronic Esters: Catalytic Studies and Stoichiometric Model Reactions on the Transmetallation Step. *Chem. - Eur. J.* **2017**, *23*, 12218−12232. (q) Thomas, A. A.; Zahrt, A. F.; Delaney, C. P.; Denmark, S. E. Elucidating the Role of the Boronic Esters in the Suzuki−Miyaura Reaction: Structural, Kinetic, and Computational Investigations. *J. Am. Chem. Soc.* **2018**, *140* (12), 4401−4416.

(6) Computational mechanistic studies about Pd-catalyzed S-M coupling: (a) Goossen, L. J.; Koley, D.; Hermann, H. L.; Thiel, W.

https://doi.org/10.1021/acs.organomet.1c00090
Organometallics 2021, 40, 1120−1128

The Palladium-Catalyzed Cross-Coupling Reaction of Carboxylic Anhydrides with Arylboronic Acids: A DFT Study. *J. Am. Chem. Soc.* **2005**, *127* (31), 11102−11114. (b) Braga, A. A. C.; Morgon, N. H.; Ujaque, G.; Maseras, F. Computational Characterization of the Role of the Base in the Suzuki−Miyaura Cross-Coupling Reaction. *J. Am. Chem. Soc.* **2005**, *127* (25), 9298−9307. (c) Goossen, L. J.; Koley, D.; Hermann, H. L.; Thiel, W. Palladium Monophosphine Intermediates in Catalytic Cross-Coupling Reactions: A DFT Study. *Organometallics* **2006**, *25* (1), 54−67. (d) Braga, A. A. C.; Ujaque, G.; Maseras, F. A DFT Study of the Full Catalytic Cycle of the Suzuki−Miyaura Cross-Coupling on a Model System. *Organometallics* **2006**, *25* (15), 3647−3658. (e) Lakmini, H.; Ciofini, I.; Jutand, A.; Amatore, C.; Adamo, C. Pd-Catalyzed Homocoupling Reaction of Arylboronic Acid: Insights from Density Functional Theory. *J. Phys. Chem. A* **2008**, *112* (50), 12896−12903. (f) Huang, Y.-L.; Weng, C.-M.; Hong, F.-E. Density Functional Studies on Palladium-Catalyzed Suzuki−Miyaura Cross-Coupling Reactions Assisted by N- or P-Chelating Ligands. *Chem. -Eur. J.* **2008**, *14* (14), 4426−4434. (g) Jover, J.; Fey, N.; Purdie, M.; Lloyd-Jones, G. C.; Harvey, J. N. A computational study of phosphine ligand effects in Suzuki−Miyaura coupling. *J. Mol. Catal. A: Chem.* **2010**, *324* (1), 39−47. (h) Kozuch, S.; Martin, J. M. L. What Makes for a Bad Catalytic Cycle? A Theoretical Study on the Suzuki−Miyaura Reaction within the Energetic Span Model. *ACS Catal.* **2011**, *1* (4), 246−253. (i) Kozuch, S.; Martin, J. M. L. What makes for a good catalytic cycle? A theoretical study of the SPhos ligand in the Suzuki−Miyaura reaction. *Chem. Commun.* **2011**, *47* (17), 4935−4937. (j) García-Melchor, M.; Braga, A. A. C.; Lledós, A.; Ujaque, G.; Maseras, F. Computational Perspective on Pd-Catalyzed C−C Cross-Coupling Reaction Mechanisms. *Acc. Chem. Res.* **2013**, *46* (11), 2626−2634. (k) Ortuño, M. A.; Lledós, A.; Maseras, F.; Ujaque, G. The Transmetalation Process in Suzuki−Miyaura Reactions: Calculations Indicate Lower Barrier via Boronate Intermediate. *ChemCatChem* **2014**, *6* (11), 3132−3138. (l) Audran, G.; Brémond, P.; Marque, S. R. A.; Siri, D.; Santelli, M. Calculated linear free energy relationships in the course of the Suzuki−Miyaura coupling reaction. *Tetrahedron* **2014**, *70* (13), 2272−2279. (m) Yaman, T.; Harvey, J. N. Suzuki−Miyaura coupling revisited: an integrated computational study. *Faraday Discuss.* **2019**, *220* (0), 425−442.

(7) Mechanistic studies about Ni-catalyzed S-M coupling: (a) Zhang, K.; Conda-Sheridan, M.; Cooke, S. R.; Louie, J. N-Heterocyclic Carbene Bound Nickel(I) Complexes and Their Roles in Catalysis. *Organometallics* **2011**, *30* (9), 2546−2552. (b) Christian, A. H.; Müller, P.; Monfette, S. Nickel Hydroxo Complexes as Intermediates in Nickel-Catalyzed Suzuki−Miyaura Cross-Coupling. *Organometallics* **2014**, *33* (9), 2134−2137. (c) Payard, P.-A.; Perego, L. A.; Ciofini, I.; Grimaud, L. Taming Nickel-Catalyzed Suzuki-Miyaura Coupling: A Mechanistic Focus on Boron-to-Nickel Transmetalation. *ACS Catal.* **2018**, *8* (6), 4812−4823.

(8) Diphosphine monoxide ligands have recently attracted much attention and proved crucial in some chemical transformations: (a) Grushin, V. V. Mixed Phosphine−Phosphine Oxide Ligands. *Chem. Rev.* **2004**, *104* (3), 1629−1662. (b) Li, H.; Belyk, K. M.; Yin, J.; Chen, Q.; Hyde, A.; Ji, Y.; Oliver, S.; Tudge, M. T.; Campeau, L.-C.; Campos, K. R. Enantioselective Synthesis of Hemiaminals via Pd-Catalyzed C−N Coupling with Chiral Bisphosphine Mono-oxides. *J. Am. Chem. Soc.* **2015**, *137* (41), 13728−13731. (c) Ji, Y.; Li, H.; Hyde, A. M.; Chen, Q.; Belyk, K. M.; Lexa, K. W.; Yin, J.; Sherer, E. C.; Williamson, R. T.; Brunskill, A.; Ren, S.; Campeau, L.-C.; Davies, I. W.; Ruck, R. T. A rational pre-catalyst design for bis-phosphine mono-oxide palladium catalyzed reactions. *Chem. Sci.* **2017**, *8* (4), 2841−2851. (d) Ji, Y.; Plata, R. E.; Regens, C. S.; Hay, M.; Schmidt, M.; Razler, T.; Qiu, Y.; Geng, P.; Hsiao, Y.; Rosner, T.; Eastgate, M. D.; Blackmond, D. G. Mono-Oxidation of Bidentate Bis-phosphines in Catalyst Activation: Kinetic and Mechanistic Studies of a Pd/Xantphos-Catalyzed C−H Functionalization. *J. Am. Chem. Soc.* **2015**, *137* (41), 13272−13281. (e) Borrajo-Calleja, G. M.; Bizet, V.; Mazet, C. Palladium-Catalyzed Enantioselective Intermolecular Carboetherification of Dihydrofurans. *J. Am. Chem. Soc.* **2016**, *138* (12), 4014−4017. (f) Ye, J.; Mu, H.; Wang, Z.; Jian, Z. Heteroaryl Backbone Strategy in Bisphosphine Monoxide Palladium-Catalyzed Ethylene Polymerization and Copolymerization with Polar Monomers. *Organometallics* **2019**, *38* (15), 2990−2997. (g) Tereniak, S. J.; Landis, C. R.; Stahl, S. S. Are Phosphines Viable Ligands for Pd-Catalyzed Aerobic Oxidation Reactions? Contrasting Insights from a Survey of Six Reactions. *ACS Catal.* **2018**, *8* (4), 3708−3714. (h) Castanet, A. S.; Colobert, F.; Broutin, P. E.; Obringer, M. Asymmetric Suzuki cross-coupling reaction: chirality reversal depending on the palladium−chiral phosphine ratio. *Tetrahedron: Asymmetry* **2002**, *13* (6), 659−665. (i) Shimizu, I.; Matsumoto, Y.; Shoji, K.; Ono, T.; Satake, A.; Yamamoto, A. Enantioselective elimination reaction of a 6,6-membered bicyclic allylic carbonate. Importance of chirality reversal depending on the palladium-chiral phosphine ratio. *Tetrahedron Lett.* **1996**, *37* (39), 7115−7118.

(9) Using CV as an analytical technique requires the addition of extra ligand, as the oxidation of the electrogenerated Pd(0) can only be observed in the presence of excess phosphine. Otherwise, Pd(0) is not stable enough and the signal is blurred due to the formation of Pd nanoparticles; see: Jutand, A. Contribution of Electrochemistry to Organometallic Catalysis. *Chem. Rev.* **2008**, *108* (7), 2300−2347. (b) Sandford, C.; Edwards, M. A.; Klunder, K. J.; Hickey, D. P.; Li, M.; Barman, K.; Sigman, M. S.; White, H. S.; Minteer, S. D. A synthetic chemist's guide to electroanalytical tools for studying reaction mechanisms. *Chem. Sci.* **2019**, *10* (26), 6404−6422.

(10) Mower, M. P.; Blackmond, D. G. Mechanistic Rationalization of Unusual Sigmoidal Kinetic Profiles in the Machetti−De Sarlo Cycloaddition Reaction. *J. Am. Chem. Soc.* **2015**, *137* (6), 2386−2391.

(11) It is worth noting that the groups of Jutand and Hartwig previously demonstrated that $[Pd^0(dppf)_2]$ requires prior dissociation of one phosphine to undergo oxidative addition. For references, see: (a) Amatore, C.; Broeker, G.; Jutand, A.; Khalil, F. Identification of the Effective Palladium(0) Catalytic Species Generated in Situ from Mixtures of Pd(dba)2 and Bidentate Phosphine Ligands. Determination of Their Rates and Mechanism in Oxidative Addition. *J. Am. Chem. Soc.* **1997**, *119*, 5176−5185. (b) Hamann, B. C.; Hartwig, J. F. Sterically Hindered Chelating Alkyl Phosphines Provide Large Rate Accelerations in Palladium-Catalyzed Amination of Aryl Iodides, Bromides, and Chlorides, and the First Amination of Aryl Tosylates. *J. Am. Chem. Soc.* **1998**, *120*, 7369−7370. (c) Hamann, B. C.; Hartwig, J. F. Additions and Corrections to Sterically Hindered Chelating Alkyl Phosphines Provide Large Rate Accelerations in Palladium-Catalyzed Amination of Aryl Iodides, Bromides, and Chlorides, and the First Amination of Aryl Tosylates. *J. Am. Chem. Soc.* **1998**, *120*, 12706−12706. (d) Alcazar-Roman, L. M.; Hartwig, J. F.; Rheingold, A. L.; Liable-Sands, L. M.; Guzei, I. A. Mechanistic Studies of the Palladium-Catalyzed Amination of Aryl Halides and the Oxidative Addition of Aryl Bromides to $Pd(BINAP)_2$ and $Pd(DPPF)_2$: An Unusual Case of Zero-Order Kinetic Behavior and Product Inhibition. *J. Am. Chem. Soc.* **2000**, *122*, 4618−4630. (e) Alcazar-Roman, L. M.; Hartwig, J. F. Mechanistic Studies on Oxidative Addition of Aryl Halides and Triflates to $Pd(BINAP)_2$ and Structural Characterization of the Product from Aryl Triflate Addition in the Presence of Amine. *Organometallics* **2002**, *21*, 491−502.

(12) (a) Amatore, C.; Jutand, A.; M'Barki, M. A. Evidence of the Formation of Zerovalent Palladium from $Pd(OAc)_2$ and Triphenylphosphine. *Organometallics* **1992**, *11* (9), 3009−3013. (b) Amatore, C.; Carre, E.; Jutand, A.; M'Barki, M. A. Rates and Mechanism of the Formation of Zerovalent Palladium Complexes from Mixtures of $Pd(OAc)_2$ and Tertiary Phosphines and Their Reactivity in Oxidative Additions. *Organometallics* **1995**, *14* (4), 1818−1826. (c) Amatore, C.; Jutand, A.; Thuilliez, A. Formation of Palladium(0) Complexes from $Pd(OAc)_2$ and a Bidentate Phosphine Ligand (dppp) and Their Reactivity in Oxidative Addition. *Organometallics* **2001**, *20* (15), 3241−3249. (d) Ozawa, F.; Kubo, A.; Hayashi, T. Generation of Tertiary Phosphine-Coordinated Pd(0) Species from $Pd(OAc)_2$ in the Catalytic Heck Reaction. *Chem. Lett.* **1992**, *21* (11), 2177−2180.

(13) The pathways were also calculated for dppe and dppp, and the heights of the TS were always proportionate to the energetic cost of phosphine decoordination (Figure S7 in the Supporting Information).

https://doi.org/10.1021/acs.organomet.1c00090
Organometallics 2021, 40, 1120−1128

DFT calculations attested that dppf favors reductive elimination and that, accordingly, the transmetalation step remains the rate-determining step (RDS) of the catalytic cycle with such types of ligands (Figure S6). In more detail, the mono-ligated TS of RE is far higher in energy (+9.2 kcal mol^{-1}) than the bis-ligated TS (−4.8 kcal mol^{-1}). In both cases, the RE is much faster than the TM, confirming the latter to be the RDS.

(14) We observed a similar behavior in the case of [Pd^{II}(Ar)(Br)$(PPh_3)_2$] (complex **1**), in agreement with a previous report from our group, see: Perego, L. A.; Grimaud, L.; Bellina, F. Mechanistic Studies on the Palladium-Catalyzed Direct C-5 Arylation of Imidazoles: The Fundamental Role of the Azole as a Ligand for Palladium. *Adv. Synth. Catal.* **2016**, *358*, 597−609 (see the Supporting Information).

(15) Similar behavior was already observed for triphenylphosphine oxide ligated Pd(0) species, see: Denmark, S. E.; Smith, R. C.; Tymonko, S. A. Phosphine oxides as stabilizing ligands for the palladium-catalyzed cross-coupling of potassium aryldimethylsilanolates. *Tetrahedron* **2007**, *63*, 5730−5738.

(16) Frisch, R. A.; Trucks, G. W.; Schlegel, H. B.; Scuseria, G. E.; Robb, M. A.; Cheeseman, J. R.; Scalmani, G.; Barone, V.; Mennucci, B.; Petersson, G. A.; Nakatsuji, H.; Caricato, M.; Li, X.; Hratchian, H. P.; Izmaylov, A. F.; Bloino, J.; Zheng, G.; Sonnenberg, J. L.; Hada, M.; Ehara, M.; Toyota, K.; Fukuda, R.; Hasegawa, J.; Ishida, M.; Nakajima, T.; Honda, Y.; Kitao, O.; Nakai, H.; Vreven, T.; Montgomery, J. A., Jr.; Peralta, J. E.; Ogliaro, F.; Bearpark, M.; Heyd, J. J.; Brothers, E.; Kudin, K. N.; Staroverov, V. N.; Kobayashi, R.; Normand, J.; Raghavachari, K.; Rendell, A.; Burant, J. C.; Iyengar, S. S.; Tomasi, J.; Cossi, M.; Rega, N.; Millam, J. M.; Klene, M.; Knox, J. E.; Cross, J. B.; Bakken, V.; Adamo, C.; Jaramillo, J.; Gomperts, R.; Stratmann, R. E.; Yazyev, O.; Austin, A. J.; Cammi, R.; Pomelli, C.; Ochterski, J. W.; Martin, R. L.; Morokuma, K.; Zakrzewski, V. G.; Voth, G. A.; Salvador, P.; Dannenberg, J. J.; Dapprich, S.; Daniels, A. D.; Farkas, O.; Foresman, J. B.; Ortiz, J. V.; Cioslowski, J.; Fox, D. J. *Gaussian 09, Rev. A.02*; Gaussian, Inc.: 2009.

(17) Zhao, Y.; Truhlar, D. G. The M06 suite of density functionals for main group thermochemistry, thermochemical kinetics, noncovalent interactions, excited states, and transition elements: two new functionals and systematic testing of four M06-class functionals and 12 other functionals. *Theor. Chem. Acc.* **2008**, *120* (1), 215−241.

(18) (a) Hay, P. J.; Wadt, W. R. Ab initio effective core potentials for molecular calculations. Potentials for K to Au including the outermost core orbitals. *J. Chem. Phys.* **1985**, *82* (1), 299−310. (b) Hay, P. J.; Wadt, W. R. Ab initio effective core potentials for molecular calculations. Potentials for the transition metal atoms Sc to Hg. *J. Chem. Phys.* **1985**, *82* (1), 270−283.

(19) (a) Tomasi, J.; Mennucci, B.; Cammi, R. Quantum Mechanical Continuum Solvation Models. *Chem. Rev.* **2005**, *105* (8), 2999−3094. (b) Cossi, M.; Scalmani, G.; Rega, N.; Barone, V. New developments in the polarizable continuum model for quantum mechanical and classical calculations on molecules in solution. *J. Chem. Phys.* **2002**, *117* (1), 43−54.

(20) Grushin, V. V. Synthesis of Hemilabile Phosphine−Phosphine Oxide Ligands via the Highly Selective Pd-Catalyzed Mono-oxidation of Bidentate Phosphines: Scope, Limitations, and Mechanism. *Organometallics* **2001**, *20* (18), 3950−3961.

https://doi.org/10.1021/acs.organomet.1c00090
Organometallics 2021, 40, 1120−1128